Available online at www.sciencedirect.com

ScienceDirect

Ceramics International 40 (2014) 967–974

CERAMICS INTERNATIONAL

www.elsevier.com/locate/ceramint

RF sputtered tri-functional antireflective TiO_2 (arc-TiO_2) compact layer for performance enhancement in dye-sensitised solar cell

M.H. Abdullah[a,*], M. Rusop[a,b]

[a]NANO-Electronic Centre, Faculty of Electrical Engineering, Universiti Teknologi MARA (UiTM), 40450 Shah Alam, Selangor, Malaysia
[b]NANO-SciTech Centre, Institute of Science, Universiti Teknologi MARA (UiTM), 40450 Shah Alam, Selangor, Malaysia

Received 20 May 2013; received in revised form 30 May 2013; accepted 24 June 2013
Available online 2 July 2013

Abstract

A novel antireflective TiO_2 compact layer (arc-TiO_2) that can reduce electron recombination and improve transmittance was deposited by RF magnetron sputtering at the interface between indium tin oxide and porous-TiO_2layer of a dye-sensitised solar cell (DSSC). Effects of the arc-TiO_2 thicknesses on the performance of the arc-TiO_2-based DSSC were investigated by means of incident photon-to-current efficiency (IPCE), open-circuit voltage decay (OCVD) and electrochemical impedance spectroscopy (EIS). The sensitisation effect of N719 dye was remarkably improved due to relatively higher and red-shifted transmittance spectra of the ITO/arc-TiO_2 electrode in a specific region, and evidenced by the IPCE measurement. Meanwhile, the slow decay behaviours of the photo-voltage owed to the compact layer were verified by the OCVD measurement. The adhesion enhancement between the arc-TiO_2 film and porous-TiO_2 layer decreases the interfacial resistance R_1 in the EIS measurement, hence facilitating the charge transfer process of the electrons in the DSSC. A significant improvement in the overall solar energy-to-electrical conversion efficiency, which constituted almost 50% higher compared with the uncoated ITO cell, is mainly attributed to the higher transmittance and reduced recombination of the arc-TiO_2 film employed as the tri-functional compact layer in the DSSC.

Keywords: Compact layer; Sensitisation effect; Recombination; Dye-sensitised solar cell

1. Introduction

Dye-sensitised solar cells (DSSC) have attracted attention because of their low-cost and high energy-conversion efficiency [1,2]. A typical DSSC consists of a nanocrystalline TiO_2 (nc-TiO_2) film covered by a monolayer of dye molecules, electrolyte, and counter-electrode. Maximum efficiencies of up to 11% have been reported so far [3]. Although intensive research efforts have been focused on DSSC, there are still challenges to be met in order to improve the overall cell efficiency of the DSSC. For instance, issues including light scattering in the TiO_2 matrix, electron generation, transfer/transport in the semi-conductor, and electron recombination have been studied in the past few decades [4,5].

Among the most studied issues in DSSC are the recombination of electrons with the I_3^- in the electrolyte at the transparent conducting oxide (TCO) and higher optical transmittance requirements of more than 80%, especially in the visible region. Generally, the first issue relates to various electrode surface modifications of Sn-doped indium oxide (ITO) through the introduction of TiO_2 [6–9], ZnO [10], Al_2O_3 [11], and so on. Recently, a majority of TCO/TiO_2 interface modifications have employed compact TiO_2 (c-TiO_2) layers acting as a blocking layer to suppress the back electron transfer from the TCO to the electrolyte. In most such cases, however, the c-TiO_2 blocking layer on the TCO acts as an impediment to severely degrade the overall optical transmittance owed to the increase in the overall TCO thickness and the establishment of multilayer stacks (glass/TCO/c-TiO_2) with a mismatch of the refractive indices between the adjacent materials in contact, thus contributing to the reflection losses in the transmittance. Lee et al. [12] and Kim et al. [13] demonstrated

*Corresponding author. Tel.: +60 3 554 31883; fax: +60 3 554 43870.
E-mail addresses: abuhanifahabllh@yahoo.com, hanapiah801@ppinang.uitm.edu.my (M.H. Abdullah).

0272-8842/$ - see front matter © 2013 Elsevier Ltd and Techna Group S.r.l. All rights reserved.
http://dx.doi.org/10.1016/j.ceramint.2013.06.093

the Nb-doped TiO_2 (NTO) layer deposited by the pulsed laser deposition (PLD) technique in commercial TCOs such as F-doped tin oxide (FTO) and ITO. Unfortunately, both studies resulted in a lower transmittance (≤75%) than the bare TCO (> 80%) in the visible light region. Given that the photo-response of a DSSC is directly influenced by the number of available photons, the light interference by the multilayer stacks can influence the spectral response of the DSSC. Nevertheless, NTO is an expensive material for compact materials, and the PLD method is not the best option for industrialisation because of the high cost of the manufacturing process.

As far as higher transmittance of an electrode equipped with a compact layer is concerned. Therefore, it is essential to fine-tune the optical properties (i.e., n_{TCO} and $n_{c\text{-}TiO2}$) of the TCO/c-TiO_2 multilayer electrode as these parameters can affect the amount of receiving light and the photo-response of the fabricated DSSC. In our previous study [14], we reported the utilisation of a gradient index antireflective type compact layer (arc-ZnO:TiO_2) that enhanced the optical and electrical properties of the TCO/arc-ZnO:TiO_2 substrate. We emphasised the need for tailoring the refractive index of each layer so as to minimise the incident light loss (ILL) when light propagates through the substrate. In this issue, we report a method of increasing the optical transmittance of an ITO/arc-TiO_2 substrate in a particular wavelength region by introducing an optimal thickness of a novel tri-functional TiO_2 antireflective compact layer under ITO glass (i.e., glass/ITO/arc-TiO_2). As depicted in Fig. 1, the step-down interference of a double layer antireflection coating (DLAR) with a graded refractive index of ($n_{arc-TiO2} > n_{ITO} > n_{glass} > n_{air}$) has been adopted in developing the novel tri-functional TCO. As for a high refractive index requirement of the film, the arc-TiO_2 compact layer was deposited at room temperature by long-throw radio-frequency (RF) magnetron sputtering [15,16]. The performance improvement of the DSSC was evaluated for different TiO_2 layer thicknesses, and critical analysis of the charge transfer phenomenon was carried out by means of incident photon-to-current efficiency (IPCE), open-circuit voltage decay (OCVD) and electrochemical impedance spectroscopy (EIS).

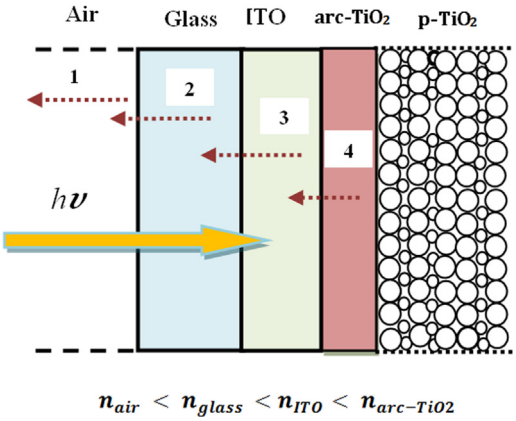

Fig. 1. Schematic diagrams of the gradient index of antireflective arc-TiO_2 compact layer DSSC.

2. Experimental procedure

2.1 Materials

Anhydrous LiI (Lithium Iodide) was obtained from Merck company. Commercially available ITO substrates were used (Samsung Corning Co. (10 Ω/□). TiO_2 powders (P-25, particle size: < 25 nm, 99.7%), Di-tetrabutylammonium *cis*-bis (isothiocyanato)*bis*(2,2′-bipyridyl-4,4′-dicarboxylato)-ruthenium (II) (N719) dyes, 4-*tert*-butyl pyridine (TBP), Polyethyleneglycol (PEG, Mw = 20,000), Iodine (I_2) and Tetrabutylammonium iodide (TBAI) were purchased from Aldrich and were used without purification.

2.2 Preparations of TiO_2 antireflective film

The antireflective films were deposited under ITO glass substrate by RF magnetron sputtering methods. The substrates were ultrasonically cleaned and degreased in acetone, rinsed in deionised water, and subsequently dried with nitrogen gas. A circular oxide target of TiO_2 (99.99% purity, 4 in. diameter, 0.25 in. thickness, Target Materials Inc.) was set up. Argon (Ar) and oxygen (O_2) were used as reactive and working gasses under the mixture ratio of (Ar:O_2) of 50:1 sccm, and the distance between the target to the substrate was 12 cm, at a constant rotating speed of 6 rpm. The chamber's working pressure was kept at 5 mTorr and a constant RF power of approximately 100 W, and the pre-sputtering was performed for 2 min.

2.3 Fabrication of DSSC devices

The preparation of porous TiO_2 film (p-TiO_2) was carried out based on mixed P25 with the TiO_2 sol–gel component reported in [17]. The TiO_2 sol–gel was mixed with 0.3 g of commercially available Degussa P-25 to avoid the cracking of the film. In order to tailor the porosity and pore sizes, the prepared paste was then added with 0.1 g of Polyethyleneglycol (PEG, Mw = 20,000) before it was subjected to ultrasonic irradiation for 10 min. The prepared p-TiO_2 paste was coated on the ITO/arc-TiO_2 substrate, dried in air at ambient temperature for 15 min. and sintered at 450 °C for 1 h. The thicknesses of the annealed films were about 10 μm, as measured using the Surface Profiler (Veeco, Dektak 150). In order to sensitise the TiO_2 electrodes, an active area of 0.25 cm^2 was selected from the sintered electrode to be immersed in 0.5 mM of N-719 dye (Ru[LL′$(NCS)_2$], L = 2,2′-bypyridyl-4,4′-dicarboxylic acid, L′ = 2,20-bypyridyl-4,40-ditetrabutylammonium carboxylate) for 24 h at 50 °C in absolute ethanol. Pt (100 nm thick) sputtered on ITO was used as an electrochemical catalyst for the counter electrode. The photo and counter electrodes were then clamped together and injected by redox electrolytes applied through a pre-drilled hole into the counter electrode. The electrolytes were composed of 0.5 M LiI, 0.05 M I_2 and 0.5 M 4-*tert*-butyl pyridine (TBP) in acetonitrile.

2.4 Measurements

The crystal structure TiO_2 electrodes were analysed by the X-ray diffraction (XRD) with Cu-Kα radiation (Rigaku-Ultima IV, (λ = 1.5405 Å)). The nanostructure and surface morphology were characterised by means of a Field Emission Scanning Electron Microscope (FE-SEM) JEOL, JSM-7600F to investigate their surface and particle size. The transmittance spectra of the ITO/arc-TiO_2 substrates were measured using a UV–Vis-NIR spectrophotometer (Varian Cary, 750). The reflectance was measured using the Thin Film Analyser Filmetrics (F50, USA). The photovoltaic characteristics of the DSSC devices were measured using a Solar Simulator (150 W simulator, Bunkoh-Keiki Co. Ltd) under simulated solar light with a Xenon Lamp power supply (AM 1.5, 100 mW/cm2). The solar simulator was calibrated to a verified Si reference cell. A multimeter (Keithley) was used for the IPCE measurement. The active area of the DSSC device measured using a black mask was 0.25 cm^2. The electrochemical impedance spectra were measured with a potentiostat (Solartron 1287) equipped with a frequency response analyser (Solartron 1260), with the frequency ranging from 10^{-1} to 10^6 Hz. The magnitude of the alternating signal was 10 mV. Impedance parameters were determined by the fitting of the impedance spectrum using Z-view software. The impedance measurements were carried out at open-circuit potential under AM 1.5 1 Sun illumination.

3. Results and discussion

3.1. Characterisation of the ITO/arc-TiO_2 substrate

Surface morphology of the deposited TiO_2 thin film as shown in Fig. 2(a) clearly shows the compact TiO_2 surface uniformly coated on the ITO side of the substrate. It provided good adhesion for the nc-TiO_2 layer in the later process, where improvement of the adhesion improved electrical contact and thereby resulted in a decrease in R_1 resistance. It has been reported that R_1 is related to electrical contact between conducting substrate and nc-TiO_2 [18,19]. In long-throw sputtering process, only the sputtered particles propagating along the paraxial directions will be deposited on the substrate, leading to the dense and homogeneous surface morphology seen in FE-SEM images. The cross-sectional image of Fig. 2(b)

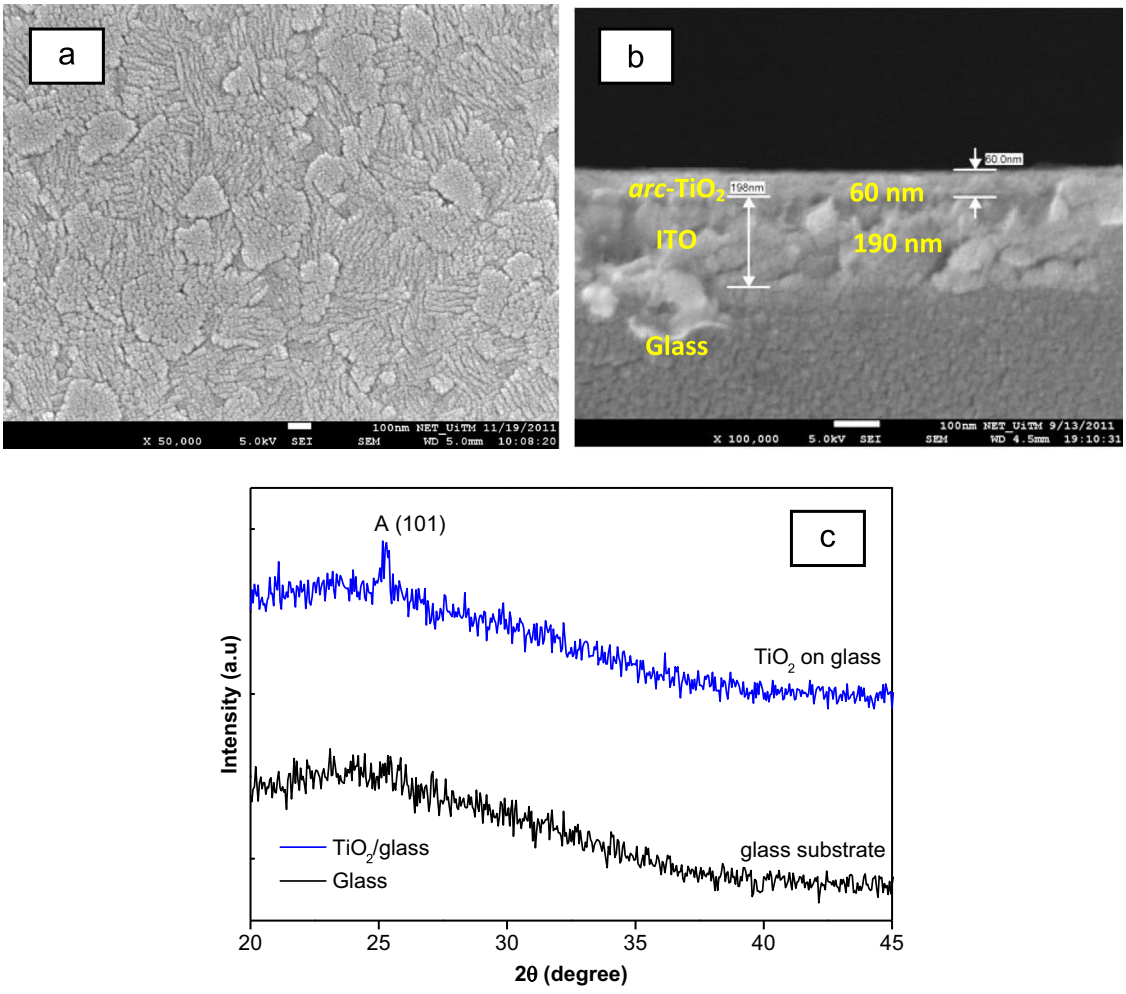

Fig. 2. (a) FE-SEM surface morphology of arc-TiO_2 electrodes, (b) cross-sectional image of the glass/ITO/arc-TiO_2 substrate, and (c) XRD pattern of the TiO_2 compact layer on glass slide.

evidences the multilayer structure with 60 nm thick arc-TiO_2 film uniformly coated on the 190 nm thick ITO. Fig. 2(c) shows the XRD pattern of the sputtered (arc-TiO_2) film deposited on a glass substrate. The film obtained after the 450 °C annealing process in air had an anatase phase.

Fig. 3 shows the transmittance spectra of the bare ITO (i.e., annealed 450 °C) and ITO/arc-TiO_2 substrate as a function of TiO_2 thicknesses. The ITO/arc-TiO_2 electrode exhibits higher transmittance than the bare ITO and FTO substrate over the entire visible range of 300–800 nm. It is one of the desirable features of the electrodes where the transmittance is improved even with an additional layer grown on the ITO. It compensates for the effect of increasing the thickness of the total substrate. Some transmittance oscillations could be observed due to the interference effect of the TiO_2 film on the ITO. Moreover, the transmittance has been red-shifted and overshot at two peaks at around 410 nm and 700 nm. The spectral response in this wavelength range is of particular interest for the N719 dye which mainly absorbs the inciden light between 400 to 600 nm range [20]. The maximum transmittance of 84% at 410 nm is observed in the first peak for the ITO/arc-TO_2, whereas the transmittance of the bare ITO shows only 80% at 370 nm. A similar transmittance of 90% could be seen in their second peak at 650 nm and 600 nm, respectively. Although a slightly lower transmittance in the 480 nm wavelength region was observed for most of the ITO/arc-TiO_2 electrodes, it was not a significant issue for transmittance because the lower transmittance will be compensated by the higher transmittance in the corresponding two peaks at 410 nm and 650 nm; in addition to that, the absorption characteristic of the N719 dye that can absorb light with wavelengths of up to 750 nm [21].

The refractive index spectra of the TiO_2 thin films are shown by the inset in Fig. 3. It can be seen that the increases of the TiO_2 film thickness have caused marginal variations of the refractive index (i.e., $n_{arc\text{-}TiO2}$) alternately ranging from 2.16 up to 2.20. It is important to control the optical thickness and refractive index (i.e., $n_{arc\text{-}TiO2}$, $d_{arc\text{-}TiO2}$ in this study) of the layers since the interference of the incident light with the multilayer substrate is affected by these two parameters [22,23], and hence changes the transmittance of the multilayer substrate. This is in good agreement with the variations of the transmittance spectra of the ITO/arc-TiO_2 substrate owed to the different thicknesses of the arc-TiO_2 film. It is worth noting that the refractive index of the ITO glass (i.e., 1.78) is still below the ITO/arc-TiO_2 samples. This indicates that the gradient refractive index of ($n_{arc-Tio2} > n_{ITo} > n_{glass} > n_{air}$) has been successfully tailored and is an effective means to reduce internal reflection in this multilayered conducting substrate with blocking layer capability.

3.2. Effect of the arc-TiO_2 blocking layer on the performance of DSSC

In order to find the optimum thickness of arc-TiO_2 compact layer. The photocurrent density–voltage characteristic for DSSCs with 60 nm, 80 nm, 100 nm and 120 nm thicknesses in comparison with a cell fabricated on an uncoated TCO substrate (ITO/nc-TiO_2) were investigated, and their curves are shown in Fig. 4. A summary of their photovoltaic characteristics is provided in Table 1. The DSSC with a 100 nm arc-TiO_2 compact layer thickness exhibits the highest short-circuit photocurrent density, J_{SC}, far better than the uncoated DSSC. In the case of the 120 nm thick compact layer, however, a further increment in the thickness did not lead to an increment of photocurrent density. It could be seen that the overall efficiency degrades after the introduction of its optimum thickness at 100 nm. Possible reasons are the increased resistance of the compact layer itself that impedes electron transport from the p-TiO_2 to the ITO [24,25], and there are more possible trap states existing in the thicker TiO_2 compact layer that tend to block the pathway of photo-excited electrons from the nc-TiO_2 layer to the ITO electrode [26,27]. Therefore, the 100 nm is considered as the most effective thickness of the compact layer, whereby there exist a balance between the rectifying properties and the electron transport properties when it is applied to the DSSC.

As a result, the highest increment in the overall quantum conversion efficiency (η) of 3.445%, almost 50% higher

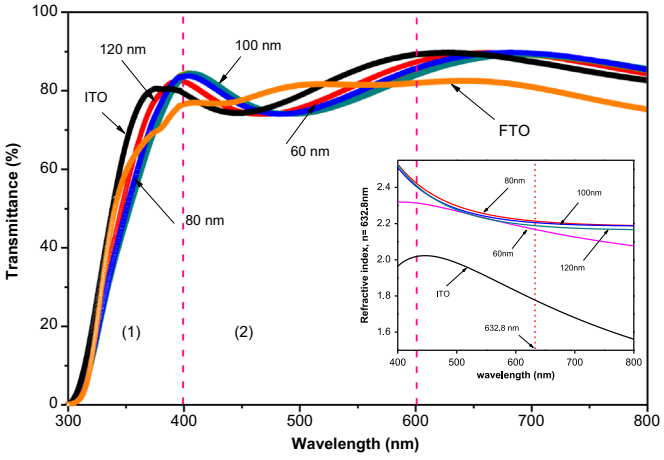

Fig. 3. Transmittance spectra, and (inset) refractive index spectra of the ITO/arc-TiO_2 substrate, at different arc-TiO_2 film thicknesses.

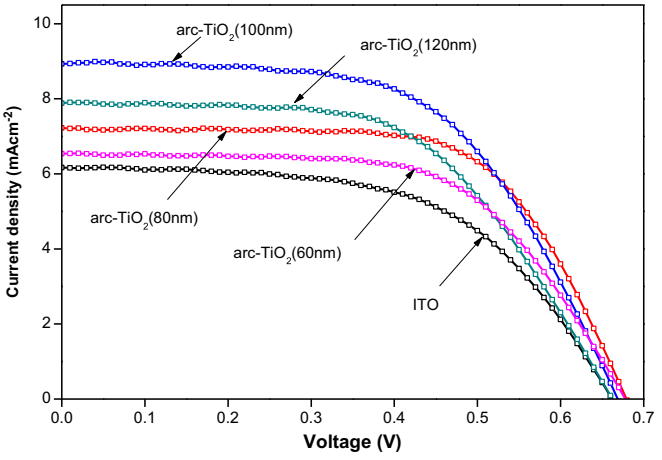

Fig. 4. Current density–voltage characteristics of DSSC at different arc-TiO_2 compact layer thicknesses.

Table 1
Comparative performances of DSSC devices fabricated using four (4) different arc-TiO_2 electrodes thicknesses under light density: 100 mW cm^{-2}:AM 1.5.

Types of photoelectrode	Open-circuit voltage, V_{OC} (V)	Short circuit current, J_{SC} (mA cm^{-2})	Fill factor (FF)	Efficiency (%)
ITO/nc-TiO_2	0.662	6.167	0.565	2.305
ITO/arc-TiO_2 (60 nm)	0.678	6.535	0.607	2.690
ITO/arc-TiO_2 (80 nm)	0.679	7.226	0.646	3.169
ITO/arc-TiO_2 (100 nm)	0.669	8.930	0.577	3.445
ITO/arc-TiO_2 (120 nm)	0.662	7.886	0.566	2.957

with respect to the standard uncoated TCO-based cell, was produced with the 100 nm thick arc-TiO_2 compact layer. As commonly reported, approximately $\pm 30\%$ increments in the overall efficiency could be achieved with the introduction of the TiO_2 compact layer to the DSSC [7,28,29]. It is, however, believed that the remarkable improvement of the overall efficiency in this study can be ascribed to three factors. The first factor is the higher and red-shifted transmittance peak of the ITO/arc-TiO_2 substrate to the 410 nm and 700 nm regions, the domain by which the N719 dye is mainly absorbed. On the other hand, the transmittance peak of the bare ITO lies at 370 nm; wavelengths lower than 390 nm are mainly affected by the absorption of TiO_2 nanoparticles [30]. The second factor is the reduction of the electron recombination at the interfaces between the TCO substrate and the electrolytes. The reduced recombination leads to the accumulation of electrons on the conduction band that causes the upward shift of the electron quasi-Fermi level E_{Fn}, thereby resulting in the improvement of the open-circuit voltage [31], and this situation is in good agreement with the improvement of the open-circuit voltage observed in this study. The third factor is the improvement of the adherence between the ITO and the nc-TiO_2 layer, by which the interfacial charge resistance (R_1) is reduced. These combined effects significantly improved the overall performance of the ITO/arc-TiO_2-based DSSC.

3.3. Incident photon-to-current efficiency

The IPCE is defined as the ratio of the number of electrons in the external circuit produced by an incident photon at a given wavelength. Any modifications made with regard to enhancing the transmittance in the cell will directly influence the IPCE. Therefore, it is believed that the improvement in the light coupling to the cell via the antireflection structure will also improve the electrons produced in the circuit. In order to investigate the light harvesting effect of the blocking layer, IPCE measurements on various arc-TiO_2-based DSSC were performed and the results are as shown in Fig. 5. It can be seen that the IPCE spectra somehow mimic the transmittance behaviour. The bare ITO cell exhibits a small shoulder at wavelength 370 nm (i.e., region-[i]) which corresponds to the first peak in the transmittance spectra of the uncoated-ITO substrate. It is often seen that the IPCE below the 390 nm region (left region) is associated with the absorption from the

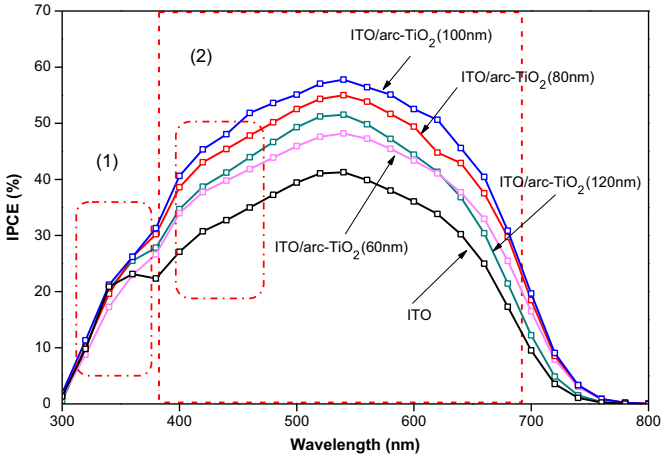

Fig. 5. IPCE spectra as a function of wavelength for the DSSC at different thicknesses of arc-TiO_2 film and bare ITO.

band-gap of the TiO_2 nanoparticles [30]. The sensitisation effect in the lower region, however, is less significant for the IPCE of the DSSC because only 2–3% of the sunlight (in the UV spectrum) can be utilised [32]. This situation devalues the effect of the transmittance spectra if the main peak lies in this region. Most importantly, the IPCE spectrum of the DSSC is primarily governed by the absorption spectrum of the dye. Therefore, it is an advantage if the first peak can be red-shifted to a longer wavelength than the 390 nm region (i.e., region-[ii]), where the N719 dye mainly absorbs and a much higher sensitisation effect can be found, so higher levels of IPCE could be obtained. Here all spectra exhibit their main shoulder in the 410–700 nm region, the region in which the peaks of the transmittance spectra of the arc-TiO_2 substrate were observed. There were small variations in the IPCE spectra with respect to the different arc-TiO_2 thicknesses, which is in good agreement with the transmittance spectra of the arc-TiO_2 substrate. The highest IPCE is obtained with the introduction of a 100 nm thick arc-TiO_2 as the cell's compact layer. Consequently, it can be concluded that the effectiveness of the light coupling to the cell is one of the factors that increases the IPCE, which was attained with the inclusion of a 100 nm thick antireflective type of compact layer (i.e., arc-TiO_2) in the DSSC.

3.4. Electrochemical impedance spectroscopy

Electrochemical impedance spectroscopy analysis was used to investigate electron transport and recombination in the

DSSC. Fig. 6 shows the EIS spectra of the DSSC fabricated from five different photo-electrodes. In the Nyquist plots, there are two sets of semicircles, each set comprises of a small semicircle at high frequency and a large semicircle at low frequency. According to the EIS model reported in the literature [33,34], the small semicircle in the frequency range of 10^3–10^5 Hz ($\omega 1$) can be ascribed to the charge transport at the ITO/TiO_2 and Pt counter electrode/electrolyte interfaces (Z_1), and the large semicircle in the low-frequency region is related to the electron transport within the p-TiO_2 layer and across the TiO_2/electrolyte interface (Z_2). The small semicircle is fitted to a charge transfer resistance (R_1) and a constant phase (Q_1), and the large semicircle is fitted to a transport resistance (R_2) and a constant phase (Q_2) [34]. The fitted parameters including R_1 and R_2 obtained by Z-view software are tabulated in Table 2. Since an identical Pt counter electrode was employed for both devices, the change at the interface of ITO/TiO_2 was mainly responsible for the difference in the R_1. As shown in Table 2, the cell with the 100 nm arc-TiO_2 compact layer exhibited the lowest values for R_1 and R_2 resistances at 2.63 Ω and 11.07 Ω, respectively. This indicates that a more efficient charge transfer process takes place at the interfaces of the ITO/arc-TiO_2 because of the enhanced interfacial adhesion. Furthermore, the electron lifetime for the recombination (τ_e) of the DSSC is determined by f_{max} values [35], where

$$\tau_e = 1/\omega_{max} \tag{1}$$

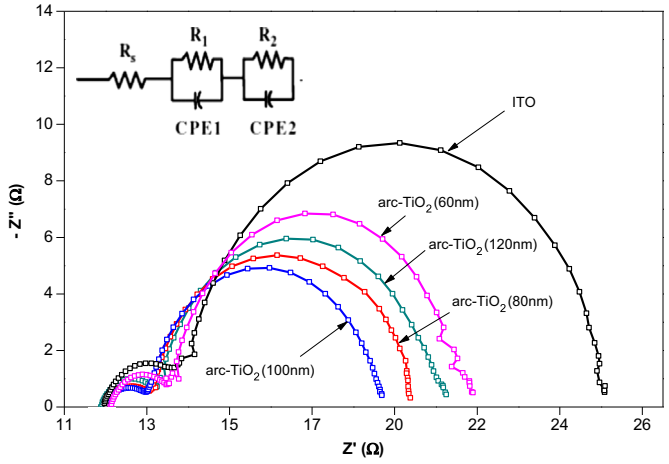

Fig. 6. EIS spectra of the DSSC as a function of TiO_2 compact layer thickness in comparison to its absence.

According to the trend shown in Table 2, the low characteristic peak of the charge transfer process at the interface of 6.746 Hz is shown by the cell with the 100 nm arc-TiO_2 compact layer. The peak frequency position is shifted to a lower region, which again indicates the reduced recombination rate at the ITO/electrolyte interface [36]. Therefore, the much reduced R_1 and R_2 after deposition of the TiO_2 thin film are the additional advantages of the arc-TiO_2 compact layer investigated in this study.

3.5. Open-circuit voltage decay

Open-circuit voltage decay analysis was conducted by monitoring the subsequent decay of the open-circuit voltage after interrupting the illumination on the DSSC under open-circuit conditions [37]. Through this technique, the gradual loss of photo-generated electrons because of recombination can be monitored by measuring the transient decay of the cell voltage after switching off the light. The decay of the photo-voltage reflects the decrease of the electron concentration at the ITO surface, which is mainly caused by the charge recombination. This means that the recombination rate of the photoelectron is proportional to the response of the OCVD. Fig. 7(a) shows the OCVD curve for DSSC with various arc-TiO_2 compact layer thicknesses in comparison with the uncoated DSSC. The slow decay component of the photo-voltage decay in all cells equipped with the arc-TiO_2 film strongly suggests the importance of such compact layers. The most effective blocking effect could be seen with the 100 nm arc-TiO_2 compact layer, which eventually gives rise to the collected current density at the external circuit. It maintains the photo-voltages for a longer time because of the accumulation of electrons in the conduction bands. It could be seen that the initial rapid decay of the photo-voltage is much less sensitive to their presence. This shows that the lowering of the quasi-Fermi level in the uncoated cells occurs via the exposed ITO substrate and the photo-voltage decay replicates the decrease in the electron concentration in the conduction band of the p-TiO_2 particles immediately next to the substrate contact [38]. Electron lifetime (τ_n) was proposed to quantify the extent of the electron recombination with the redox electrolyte and was proven effective. It was calculated using [39]

$$\tau = \frac{kT}{e}\left(\frac{dV}{dt}\right)^{-1} \tag{2}$$

Fig. 7(b) compares the dependence of the electron lifetime (τ_n) on the open-circuit voltage for DSSC with different

Table 2
Fitted results of EIS analysis for DSSC with various TiO_2 compact layer thicknesses in comparison to the bare cell.

Types of photoelectrode	R_1 (Ω)	R_2 (Ω)	f_{max} of Z_2 (Hz)	τ_e (s)
ITO/nc-TiO_2	4.45	19.43	8.196	0.019
ITO/arc-TiO_2 (60 nm)	3.57	15.35	7.273	0.022
ITO/arc-TiO_2 (80 nm)	2.75	12.97	6.887	0.023
ITO/arc-TiO_2 (100 nm)	2.63	11.07	6.746	0.024
ITO/arc-TiO_2 (120 nm)	3.11	13.36	7.104	0.022

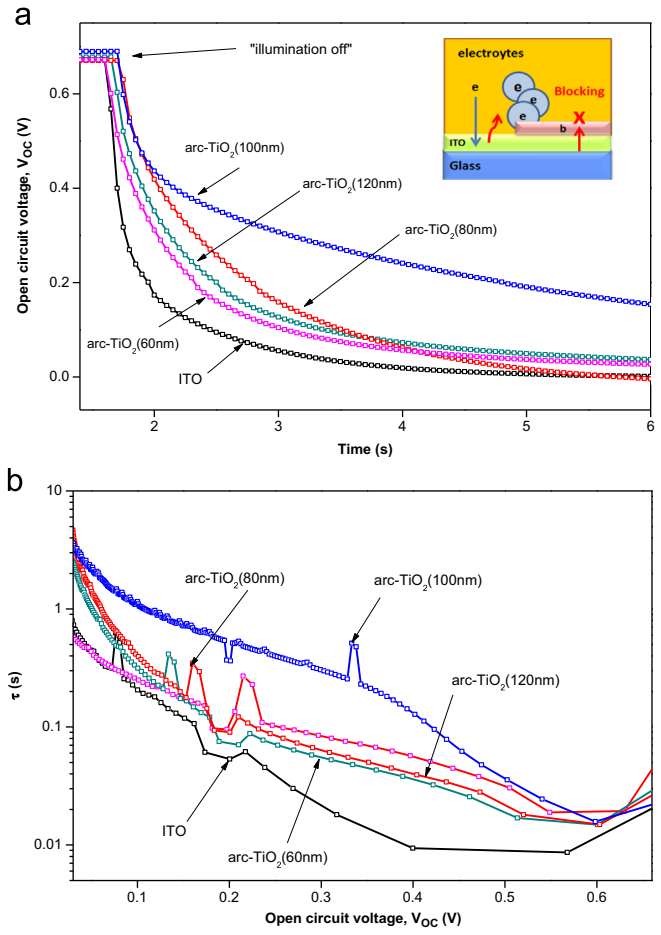

Fig. 7. (a) Open-circuit voltage decay and (b) electron lifetime (in log-linear representation) for the DSSC with various thicknesses of ITO/arc-TiO_2 compact layer

thicknesses of the arc-TiO_2 compact layer. It clearly demonstrates that, with any given open-circuit potential, the electron lifetime of the cell with the compact film is longer than that of the uncoated ITO substrate. The electron carrier lifetime of the 100 nm arc-TiO_2 compact layer is approximately five times higher than that of the bare cell at all voltages. Since the dye adsorption is negligible, the difference in the OCVD levels was mainly owed to the blocking effect of the arc-TiO_2 compact layer that makes the photo-voltage decay for a longer period. As a consequence of the slower decay, a sensible increase in the electron lifetime can be demonstrated for the cell with the compact layer. This suggests that the electrons injected from the excited dye can survive longer and hence facilitate net electron transport without undergoing losses at the surface of the ITO. This is because the longest electron lifetime for recombination could favour the highest charge collection rate of photo-generated electrons [33], which leads to the highest efficiency of the compact layer-based DSSC.

4. Conclusion

In summary, we have demonstrated a novel tri-functional antireflective TiO_2 compact layer deposited by RF magnetron sputtering. The electrochemical characteristics of the arc-TiO_2-based DSSC were examined by measuring the IPCE, OCVD and EIS. The tri-functional TiO_2 compact layer at the interface provides several good effects such as, higher red-shifted transmittance peak that favours the N719 absorption region, suppressed the back electron recombination from the ITO to the electrolyte, and reduced the interfacial charge resistance as a result of better adhesion between the surface of the ITO and the porous-TiO_2 film. These integrated features of the 100 nm thickness antireflective TiO_2 compact layer greatly improved the overall performance of the arc-TiO_2-based DSSC from 2.305% to 3.445%, which constituted an almost 50% increment compared with that of the uncoated ITO cell.

Acknowledgements

The author would like to thank Universiti Teknologi MARA (UiTM), Malaysia, and the Malaysian government for their support and funding. This work was financially supported by Universiti Teknologi MARA under Grant 600-RMI/ST/DANA5/3/Dst (19/2010). The author thanks the Mechanical Engineering Department (UiTM) for XRD measurements. Last, but not least, thanks are expressed to Mat Tamisi Zainuddin of Advanced Material Research (AMREC) Sirim, Malaysia, for optical measurements.

References

[1] B. O'Regan, M. Gratzel, A low-cost, high-efficiency solar cell based on dye-sensitized colloidal TiO_2 films, Nature 353 (1991) 737.
[2] M. Gratzel, Solar energy conversion by dye-sensitized photovoltaic cells, Inorganic Chemistry 44 (2005) 6841.
[3] M.A. Green, K. Emery, Y. Hishikawa, W. Warta, Solar cell efficiency tables (version 37), Progress in Photovoltaics: Research and Applications 19 (2011) 84–92.
[4] Gratzel, Photochemical cells, Nature 414 (6861) (2001) 338–344.
[5] S.J. Wu, H.W. Han, Q.D. Tai, J. Zhang, S. Xu, C.H. Zhou, Y. Yang, H. Hu, B.L. Chen, X.-Z. Zhao, Improvement in dye-sensitized solar cells employing TiO_2 electrodes coated with Al_2O_3 by reactive direct current magnetron sputtering, Journal of Power Sources 182 (2008) 119–124.
[6] Suk In Noh, Kokn-Nara Bae, Hyo-Jin Ahn, Tae-Yeon Seong, Improved efficiency of dye-sensitized solar cells through fluorine-doped TiO_2 blocking layer, Ceramics International, in press. ⟨http://dx.doi.org/10.1016/j.ceramint.2013.03.082⟩.
[7] Y.S. Jin, K.H. Kim, W.J. Kim, K.U. Jang, H.W. Choi, The effect of RF-sputtered TiO2 passivating layer on the performance of dye sensitized solar cells, Ceramics International 38 (2012) S505–S509.
[8] C. Rho, Ji.H. Min, J.S. Suh, Barrier layer effect on the electron transport of the dye-sensitized solar cells based on TiO2 nanotube arrays, Journal of Physical Chemistry C 116 (2012) 7213–7218.
[9] J. Kim, H. Choi, C. Nahm, J. Moon, C. Kim, S. Nam, D.R. Jung, B. Park, The effect of a blocking layer on the photovoltaic performance in CdS quantum-dot-sensitized solar cells, Journal of Power Sources 196 (2011) 10526–10531.
[10] N. Huang, Y. Liu, T. Peng, X. Sun, B. Sebo, Q. Tai, H. Hu, B. Chen, S. Guo, X. Zhao, Synergistic effects of ZnO compact layer and $TiCl_4$ post-treatment for dye-sensitized solar cells, Journal of Power Sources 204 (2012) 257–264.
[11] S.J. Wu, H.W. Han, Q.D. Tai, J. Zhang, S. Xu, C.H. Zhou, Y. Yang, H. Hu, B.L. Chen, X.Z. Zhao, Journal of Power Sources 182 (1) (2008) 119.
[12] S. Lee, J.H. Noh, H.S. Han, D.K. Yim, D.H. Kim, J.K. Lee, J.Y. Kim, H.S. Jung, K.S. Hong, Nb-doped TiO : a new compact layer material for

TiO dye-sensitized solar cells, Journal of Physical Chemistry C 113 (2009) 6878–6882.
[13] D.H. Kim, S.W. Lee, J.H. Park, J.H. Noh, I.J. Park, W.M. Seong, K.S. Hong, Transmittance optimized nb-doped TiO2/Sn-doped In_2O_3 multilayered photoelectrodes for dye-sensitized solar cells, Solar Energy Materials & Solar Cells 96 (2012) 276–280.
[14] M.H. Abdullah, L.N. Ismail, M.H. Mamat, M.Z. Musa, M. Rusop, Novel encapsulated ITO/arc-ZnO:TiO_2 antireflective passivating layer for TCO conducting substrate prepared by simultaneous radio frequency-magnetron sputtering, Microelectronic Engineering 108 (2013) 138–144.
[15] M.J. Chuang, H.F. Huang, C.H. Wen, A.K. Chu, On the structure and surface chemical composition of indium–tin oxide films, Thin Solid Films 518 (2010) 2290–2294.
[16] R.V. Joshi, S. Brodsky, Collimated sputtering of TiN/Ti liners into sub-half-micrometer high aspect ratio contacts/lines, Applied Physics Letters 61 (1992) 2613–2615.
[17] L. Zhang, Y. Zhu, Yu He, Wei Li, H. Sun, Preparation and performances of mesoporous TiO_2 film photocatalyst supported on stainless steel, Applied Catalysis B: Environmental 40 (2003) 287–292.
[18] T. Hoshikawa, M. Yamada, R. Kikuchi, K. Eguchi, Impedance analysis of internal resistance affecting the photoelectrochemical performance of dye-sensitized solar cells, Journal of The Electrochemical Society 152 (2005) E68.
[19] N.-G. Park, K.M. Kim, M.G. Kang, K.S. Ryu, S.H. Chang, Y.-J. Shin, Chemical sintering of nanoparticles: a methodology for low-temperature fabrication of dye-sensitized TiO_2 films, Advanced Materials 17 (2005) 2349.
[20] M.K. Nazeeruddin, R. Humphry-Baker, P Liska, M Gratzel, Investigation of sensitizer adsorption and the influence of protons on current and voltage of a dye-sensitized nanocrystalline TiO_2 Solar cell, Journal of Physics and Chemistry B107 (2003) 8981–8987.
[21] Y.J. Kim, Y.H. Lee, M.H. Lee, H.J. Kim, J.H. Pan, G.I. Lim, Y.S. Choi, K. Kim, N.G. Park, C. Lee, W.I. Lee, Formation of efficient dye-sensitized solar cells by introducing an interfacial layer of long-range ordered mesoporous TiO_2 thin film, Langmuir 24 (2008) 13225–13230.
[22] D. Mardare, G.I. Rusu, On the structure and optical dielectric constant of TiO2 sputtered thin films, Journal of Optoelectronics and Advanced Materials M3 (2001) 95–100.
[23] D Mardare, E. Apostol, TiO_2 thin films doped by Ce, Nb, Fe, deposited onto ITO/glass substrates, Journal of Optoelectronics and Advanced Materials M8 (2006) 914–916.
[24] L. Mora-Sero, S. Gimenez, F. Febregat-Santiago, R. Gomez, Q. Shen, T. Toyoda, J. Bisquert, Recombination in quantum dot sensitized solar cells, Accounts of Chemical Research 42 (2009) 1848–1857.
[25] S.M. Waita, B.O. Aduda, J.M. Mwabora, G.A. Niklasson, C.G. Granqvist, G. Boschloo, Electrochemical characterization of TiO2 blocking layers prepared by reactive DC magnetron sputtering, Journal of Electroanalytical Chemistry 637 (2009) 79–83.
[26] Z. Zhang, S.M. Zakeeruddin, B. O'Regan, R. Humphry-Baker, M. Grätzel, Influence of 4-guanidinobutyric acid as coadsorbent in reducing recombination in dye-sensitized solar cells, Journal of Physical Chemistry B 109 (2005) 21818–21824.
[27] T. Berger, T. Lana-Villarreal, D. Monllor-Satoca, R. Gómez, An electrochemical study on the nature of trap states in nanocrystalline rutile thin films, Journal of Physical Chemistry C 111 (2007) 9936–9942.
[28] Michele Manca, Francesco Malara, Luigi Matriradonna, Luisa De Marco, Roberto Giannuzzi, Roberto Cingolani, Giuseppe Gigli. Charge recombination reduction in dye-sensitized solar cells by means of an electron beam-deposited TiO_2 buffer layer between conductive glass and photoelectrode, Thin Solid Film 518 (2010) 7147-7151.
[29] H. Yu, S. Zhang, H. Zhao, G. Will, P. Liu, An efficient and low-cost TiO_2 compact layer for performance improvement of dye-sensitized solar cells, Electrochimica Acta 54 (2009) 1319–1324.
[30] M. Gratzel, Dye-sensitized solar cells, Journal of Photochemistry and Photobiology C 4 (2003) 145–153.
[31] C.-H. Lin, S. Chattopadhyay, C.-W. Hsu, M.-H. Wu, W.-C. Chen, C.-T. Wu., S.-C Tseng, J.-S Hwang, J.-H. Lee, C.-W. Chen, C.-H. Chen, L.-C. Chen, K.-H. Chen, Enhanced charge separation by sieve-layer mediation in high-efficiency inorganic–organic solar cells, Advanced Materials 21 (2009) 759–763.
[32] Y. Lee, M. Kang, The optical properties of nanoporous structured titanium dioxide and the photovoltaic efficiency on DSSC, Journal of Industrial and Engineering Chemistry 122 (2010) 284–289.
[33] Y.Z. Zheng, X. Tao, L.X. Wang, H. Xu, Q. Hou, W.L. Zhou, J.F. Chen, Novel ZnO-based film with double light-scattering layers as photoelectrodes for enhanced efficiency in dye-sensitized solar cells, Chemistry of Materials 22 (2010) 928.
[34] J.B. Xia, N. Masaki, K.J. Jiang, S. Yanagida, Sputtered Nb_2O_5 as a novel blocking layer at conducting glass/TiO_2 interfaces in dye-sensitized ionic liquid solar cells, Journal of Physical Chemistry C 111 (22) (2007) 92.
[35] M. Adachi, M. Sakamoto, J.T. Jiu, Y. Ogata, S. Isoda, Determination of parameters of electron transport in dye-sensitized solar cells using electrochemical impedance spectroscopy, Journal of Physical Chemistry B 110 (28) (2006) 13872.
[36] R. Kern, R. Sastrawan, J. Ferber, R. Stangl, J. Luther, Modeling and interpretation of electrical impedance spectra of dye solar cells operated under open-circuit conditions, Electrochimica Acta 47 (2002) 4213–4225.
[37] A. Zaban, M. Greenshtein, J. Bisquert, Determination of the electron lifetime in nanocrystalline dye solar cells by open-circuit voltage decay measurements, ChemPhysChem 4 (2003) 859.
[38] P.J. Cameron, L.M. Peter, Characterization of titanium dioxide blocking layers in dye-sensitized nanocrystalline solar cells, Journal of Physical Chemistry B 107 (2003) 14394.
[39] J. Bisquert, A. Zaban, M. Greenshtein, I. Mora-Sero, Determination of rate constants for charge transfer and the distribution of semiconductor and electrolyte electronic energy levels in dye-sensitized solar cells by open-circuit photovoltage decay method, Journal of the American Chemical Society 126 (41) (2004) 13550.